HHS Public Access

Author manuscript

Mol Cancer Res. Author manuscript; available in PMC 2017 May 31.

Published in final edited form as:

Mol Cancer Res. 2017 March ; 15(3): 250–258. doi:10.1158/1541-7786.MCR-16-0132.

Autophagy Inhibition Enhances Sunitinib Efficacy in Clear Cell Ovarian Carcinoma

Lindsay DeVorkin[1,2], **Matthew Hattersley**[1], **Paul Kim**[1], **Jenna Ries**[1], **Jaeline Spowart**[1,2], **Michael S. Anglesio**[3], **Samuel M. Levi**[4], **David G. Huntsman**[3], **Ravi K. Amaravadi**[5], **Jeffrey D. Winkler**[4], **Anna V. Tinker**[6], and **Julian J. Lum**[1,2]

[1]Trev and Joyce Deeley Research Centre, BC Cancer Agency, Victoria, British Columbia, Canada

[2]Department of Biochemistry and Microbiology, University of Victoria, Victoria, British Columbia, Canada

[3]Department of Pathology and Laboratory Medicine, University of British Columbia, Vancouver, British Columbia, Canada

[4]Department of Chemistry, School of Arts and Science, University of Pennsylvania, Philadelphia, Pennsylvania

[5]Department of Medicine and Abramson Cancer Center, Perelman School of Medicine, University of Pennsylvania, Philadelphia, Pennsylvania

[6]BC Cancer Agency, Division of Medical Oncology, Vancouver Centre, Vancouver, British Columbia, Canada

Abstract

Clear cell ovarian carcinoma (CCOC) is an aggressive form of epithelial ovarian cancer that exhibits low response rates to systemic therapy and poor patient outcomes. Multiple studies in CCOC have revealed expression profiles consistent with increased hypoxia, and our previous data suggest that hypoxia is correlated with increased autophagy in CCOC. Hypoxia-induced

Corresponding Author: Julian J. Lum, BC Cancer Agency, 2410 Lee Avenue, Victoria, British Columbia V8R 6V5, Canada. Phone: 250-519-5718; Fax: 250-519-2040; jjlum@bccancer.bc.ca.

Note: Supplementary data for this article are available at Molecular Cancer Research Online (http://mcr.aacrjournals.org/).

Disclosure of Potential Conflicts of Interest

R.K. Amaravadi has ownership interest (including patents) in and is a consultant/advisory board member for Presage Biosciences. A.V. Tinker is a consultant/advisory board member for AstraZeneca. No potential conflicts of interest were disclosed by the other authors.

Authors' Contributions

Conception and design: L. DeVorkin, D.G. Huntsman, J.J. Lum

Development of methodology: L. DeVorkin, J. Spowart, D.G. Huntsman, J.D. Winkler, J.J. Lum

Acquisition of data (provided animals, acquired and managed patients, provided facilities, etc.): L. DeVorkin, P. Kim, J. Ries, S.M. Levi, A.V. Tinker

Analysis and interpretation of data (e.g., statistical analysis, biostatistics, computational analysis): L. DeVorkin, P. Kim, J. Ries, R.K. Amaravadi, A.V. Tinker, J.J. Lum

Writing, review, and/or revision of the manuscript: L. DeVorkin, P. Kim, J. Ries, J. Spowart, M.S. Anglesio, R.K. Amaravadi, A.V. Tinker, J.J. Lum

Administrative, technical, or material support (i.e., reporting or organizing data, constructing databases): M. Hattersley, M.S. Anglesio, R.K. Amaravadi, J.J. Lum

Study supervision: L. DeVorkin, J.J. Lum

autophagy is a key factor promoting tumor cell survival and resistance to therapy. Recent clinical trials with the molecular-targeted receptor tyrosine kinase (RTK) inhibitor sunitinib have demonstrated limited activity. Here, it was evaluated whether the hypoxia–autophagy axis could be modulated to overcome resistance to sunitinib. Importantly, a significant increase in autophagic activity was found with a concomitant loss in cell viability in CCOC cells treated with sunitinib. Pharmacologic inhibition of autophagy with the lysosomotropic analog Lys05 inhibited autophagy and enhanced sunitinib-mediated suppression of cell viability. These results were confirmed by siRNA targeting the autophagy-related gene *Atg5*. In CCOC tumor xenografts, Lys05 potentiated the antitumor activity of sunitinib compared with either treatment alone. These data reveal that CCOC tumors have an autophagic dependency and are an ideal tumor histotype for autophagy inhibition as a strategy to overcome resistance to RTK inhibitors like sunitinib.

Implications—This study shows that autophagy inhibition enhances sunitinib-mediated cell death in a preclinical model of CCOC.

Introduction

Tumor hypoxia resulting from an inadequate oxygen supply is a well-recognized mechanism driving resistance to chemotherapy and radiotherapy. Hypoxia can also activate autophagy, a pathway whereby tumors degrade intracellular contents to generate nutrients and metabolites for maintaining bioenergetics and survival (1). Pharmacologic inhibition of late-stage autophagy using lysosomotropic agents, such as chloroquine (CQ) or its derivative hydroxychloroquine (HCQ), has been shown to enhance the efficacy of antitumor agents (1). As such, phase I and II clinical trials investigating HCQ in combination with chemotherapies or targeted therapies are ongoing. Early reports have indicated that HCQ may have modest clinical activity (2–6). However, in the absence of a specific autophagy inhibitor, targeting other events upstream or downstream of autophagy may improve clinical responses. More recently a new agent, Lys05, was identified as a more potent inhibitor of autophagy (7). Preclinical studies have shown that mice treated with Lys05 phenocopy the deletion of essential autophagy genes, suggesting that it may have more specificity than other lysosomotropic drugs (7). Despite these developments, a yet unresolved and crucial issue is the identification of tumor types that are susceptible to autophagy inhibition.

Clear cell ovarian carcinoma (CCOC) is a distinct histotype of epithelial ovarian cancer that is characterized by poor response rates to platinum-based chemotherapies, especially in the advanced setting (8, 9). There is compelling genetic and molecular evidence that CCOCs activate pathways involved in hypoxia and angiogenesis (10, 11). We previously found that the presence of the autophagy marker LC3A-SLS (microtubule-associated protein 1 light chain 3A-stone like structures) in CCOC is associated with a significant reduction in survival (12). Moreover, we observed a positive correlation between LC3A-SLS and the proangiogenic proteins hypoxia-inducible factor 1-alpha (HIF-1α) and carbonic anhydrase IX (CA-IX). Taken together, these studies suggest that CCOC patient tumors are associated with activation of hypoxia-induced autophagy, and we hypothesize that CCOC may represent a unique tumor type that has inherent susceptibility to autophagy inhibition.

Sunitinib (Sutent) is a pan–receptor tyrosine kinase (RTK) inhibitor approved for the treatment of renal cell carcinoma (RCC), pancreatic neuroendocrine tumors (PNET), and imatinib-resistant gastrointestinal tumors (GIST). Sunitinib blocks the VEGF, PDGF, FLT3, and c-Kit signaling pathways and therefore has both antiangiogenic and antitumor properties. Although antiangiogenic drugs, including sunitinib, block the growth of blood vessels, it has been demonstrated that sunitinib can induce vascular normalization, increasing tumor oxygenation and suppressing cycling hypoxia (13). Because of the similarities between RCC and CCOC, it was proposed that sunitinib may also have a therapeutic role in CCOC (10, 14). Indeed, there have been case reports of sustained clinical and functional imaging responses in three chemotherapy-resistant CCOC patients treated with sunitinib (10, 15). However, the results of two phase II clinical trials indicate that although there were some durable responses in CCOC, the overall activity of sunitinib was low (16, 17).

The association between hypoxia, autophagy and treatment resistance, and the modest response to sunitinib observed in CCOC provided the rationale to investigate the synergy between sunitinib and autophagy inhibition as a potential therapeutic strategy for treating CCOCs. Our data show that autophagy inhibition enhances sunitinib efficacy under normoxia and hypoxia and that targeting the autophagy pathway may represent an efficacious strategy to enhance the benefits of sunitinib.

Materials and Methods

Cell culture and hypoxia conditions

Cells were maintained in a humidified incubator at 37°C with 5% CO_2 and were used within 20 passages. OVTOKO and OVMANA cells were obtained from the JCRB cell bank (gift from J. Brenton, University of Cambridge, Li Ka Shing Centre, Cambridge, United Kingdom) and were cultured in RPMI supplemented with 10% FBS, 2.05 mmol/L L-glutamine, 100 U/mL penicillin, and 100 μg/mL streptomycin (all from Fisher Scientific). TOV21G were obtained from ATCC and cultured in the above media with the addition of HEPES. Cells were authenticated using short tandem repeat profiling (AmpFlSTR Identifiler, Applied Biosystems) and were thawed and used within 6 months of receipt. For hypoxia experiments, cells were placed in a humidified hypoxia chamber (Coy Laboratories) at 37°C, 1% O_2 with 5% CO_2 and cultured as indicated.

Cell viability assays and combination index analysis

For viability analyses at 48 hours, 7.5×10^3 cells were plated into each well of a 96-well plate in duplicate. For 72-hour analyses, 2×10^3 (TOV21G and OVTOKO) and 3×10^3 (OVMANA) cells were plated. The following day, cells were treated with sunitinib (LC Laboratories), HCQ (Acros Organics Source), or Lys05 as indicated (7). MTT (5 mg/mL) was added to each well and was incubated for 4 hours at 37°C. MTT was then solubilized in 100 μL of DMSO (Sigma-Aldrich), and absorbance was measured at 560 and 670 nm on a VersaMAX microplate reader. IC_{50} values were calculated using GraphPad Prism 6. The combination index (CI) was determined using the median effect principle by Chou and Talalay (18). The fraction affected (Fa) was calculated by subtracting the relative viability

from 1, where Fa =1 indicates 0% viability and Fa = 0 indicates 100% viability. The CI values were determined using CompuSyn software, where a CI < 1 indicates synergistic, CI =1 indicates additive, and CI > 1 indicates antagonistic interactions.

Crystal violet cell recovery assays

A total of 500 cells/well in 24-well plates were treated with Lys05 and sunitinib for 48 hours. Media were removed and replaced with fresh media, and cells were incubated for an additional 11 days. Cells were then fixed in 10% neutral buffered formalin (Sigma-Aldrich) and stained with 0.1% (w/v) crystal violet (Sigma-Aldrich). Crystal violet was solubilized in 10% acetic acid, and absorbance was measured at 590 nm on a VersaMAX microplate reader.

siRNA

Cells were plated at 2×10^5 cells/well in 6-well plates in antibiotic-free medium. The following day, cells were transfected with scramble-siRNA, or a pool of two specific siRNAs targeting Atg5 using DharmaFECT Transfection Reagent (Dharmacon) according to the manufacturer's instructions. Forty-eight hours after transfection, cells were collected for Western blot analyses. For siRNA treatments combined with sunitinib, 5×10^3 cells were plated in duplicate in antibiotic-free media in a 96-well plate. The following day, cells were transfected with scramble or Atg5 siRNA as described above. Twenty-four hours after transfection, media were replaced with fresh media in the presence or absence of sunitinib, and cells were incubated for an additional 48 hours. For crystal violet recovery assays, siRNA-treated cells were collected 24 hours after transfection and were plated at 500 cells/well and treated as indicated above.

Caspase-Glo 3/7 assay

Cells (7.5×10^3) were plated in duplicate in a 96-well plate. The following day, cells were treated with Lys05, sunitinib, or the combination of the two agents for 48 hours. Etoposide (100 μmol/L) was used as a positive control. Caspase-3/7 activity was determined according to the manufacturer's instructions (Promega). Luminescence was measured on a Wallac EnVision multilabel reader.

Western blots

Western blots were performed as described previously (19). Primary antibodies used were anti-LC3B and GAPDH (Novus Biologicals), p62 and actin (Sigma-Aldrich), PARP, p-mTOR Ser2448, mTOR, p-S6 Ser235/236 and S6 (Cell Signaling Technology). Densitometry was performed using ImageJ software.

Xenograft studies

All animal procedures were approved by the University of Victoria Animal Care Committee and were performed in accordance with the Canadian Council on Animal Care. Female NOD/Scid mice were purchased from the BC Cancer Research Facility and housed under aseptic conditions in microisolater cages. Approximately 8-week-old NOD/Scid mice were implanted with 2×10^6 TOV21G or OVTOKO cells subcutaneously into the right flank.

Once tumors reached approximately 100 mm^3, mice were treated with PBS (daily, intraperitoneally), 20 mg/kg sunitinib (daily, oral gavage), 20 mg/kg Lys05 (daily, intraperitoneally), or the combination of the two agents for 18 (TOV21G) or 13 (OVTOKO) days. Tumor volume was measured daily with digital calipers and was calculated according to the formula $mm^3 = 0.5 \times length \times width^2$.

IHC and TOV21G tumor xenograft scoring

Formalin-fixed tissue was embedded in paraffin blocks. Tissue sections (4 μm) were subjected to antigen retrieval as described previously (20). Slides were washed and antibodies to pimonidazole (Hypoxyprobe), cleaved caspase-3 (Cell Signaling Technology), or Ki-67 (Abcam) were incubated for 30 minutes at room temperature. Following washing, rabbit horseradish peroxidase secondary antibody (Biocare) was applied, and secondary antibodies were detected using 3,3′-diaminobenzidine chromogen (DAB; Biocare). Slides were washed and allowed to air dry before mounting with EcoMount (Biocare).

Scoring of tumor tissues was performed by taking 4 to 5 high power fields at ×20 magnification using Nuance Multispectral Imaging Software in combination with an Olympus BX53 microscope. Pimonidazole and cleaved caspase-3 were scored using signal thresholding, and Ki-67–positive cells were enumerated using InForm Software Analysis.

Statistical analyses

Unless otherwise indicated, statistical analyses were determined using Student *t* test. All statistical calculations were used using GraphPad 6.0 software, and *P* values <0.05 were considered significant.

Results

CCOC cells are sensitive to sunitinib *in vitro*

We investigated the effects of sunitinib on three CCOC cell lines with respect to cell viability under normoxic (21% O_2) and hypoxic (1% O_2) conditions. Under normoxia, TOV21G, OVTOKO, and OVMANA CCOC cells showed a dose-dependent decrease in cell viability following sunitinib treatment, with an IC_{50} calculated to be 17.3, 21.1, and 18.6 μmol/L, respectively (Fig. 1A–C). At 72 hours, the IC_{50} was similar to those observed in reported studies (Supplementary Fig. S1; ref. 21). CCOC cells cultured under hypoxia for 48 hours were also sensitive to sunitinib but showed cell line–dependent differences. TOV21G cells cultured under hypoxia were the most resistant to sunitinib, with a small but reproducible 0.2-fold increased IC_{50} under hypoxia compared with normoxia. In contrast, OVTOKO and OVMANA cells were more sensitive to sunitinib under hypoxia, with IC_{50} values 0.2- and 0.7-fold less under hypoxia compared with normoxia, respectively (Fig. 1A–C).

Modulation of autophagy by sunitinib in CCOC cell lines

We previously showed that hypoxia induces autophagy in CCOC cell lines (12). Sunitinib however has been shown to induce or block autophagy depending on the cell type (22–26). To determine the effect of sunitinib on autophagy in CCOC cells, we first examined LC3-II

and the autophagy-dependent degradation of p62 following sunitinib treatment. The free cytoplasmic form of LC3 (LC3-I) becomes conjugated to phosphatidylethanolamine (LC3-II) and is recruited to autophagosomal membranes (27). Although an increase in LC3-II can reflect an increase in autophagy, an accumulation of autophagosomes may be the result of increased autophagosome biogenesis or impairment of autophagosome trafficking to lysosomes (20). We found that all three CCOC cell lines treated with increasing concentrations of sunitinib showed a significant increase in LC3-II (Fig. 2A). In addition, a significant reduction in p62 was observed for TOV21G and OVTOKO cells, whereas OVMANA cells had a modest reduction of p62 (Fig. 2A). To confirm the role of sunitinib on autophagy, autophagic flux assays were performed under both normoxia and hypoxia by treating cells with sunitinib in the presence or absence of saturating concentrations of the autophagy inhibitor Lys05 (Supplementary Fig. S2). Under normoxia, TOV21G and OVTOKO cells treated with sunitinib and Lys05 resulted in a further accumulation of LC3-II compared with single-agent sunitinib or Lys05, indicating that sunitinib induces autophagic flux in these cells (Fig. 2B). When cells were cultured under hypoxic conditions, sunitinib treatment blocked autophagic flux in TOV21G cells, while it induced flux in OVTOKO cells (Fig. 2C). In OVMANA cells cultured under normoxic or hypoxic conditions, we observed a significant increase in LC3-II in the sunitinib plus Lys05 treatment group compared with Lys05 alone, but not compared with sunitinib alone. This indicates that sunitinib induces the synthesis of autophagy-related membranes but may not induce flux in these cells (Fig. 2B and C; ref. 28). It is possible that higher concentrations of sunitinib are required to induce flux under normoxia or hypoxia in this cell line. Similar to other reports, CCOC cells treated with sunitinib led to a reduction in both phospho-mTOR and phospho-S6, indicating that sunitinib-induced autophagy involves suppression of the mTOR signaling pathway (Fig. 2D; ref. 29).

Autophagy inhibition potentiates the antitumor activity of sunitinib *in vitro*

Given the above results, it is possible that the induction as well as the magnitude of autophagy in CCOC may contribute to treatment resistance and poor outcomes. We hypothesized that targeting the autophagy pathway may sensitize CCOC to sunitinib. Lys05 is a dimeric derivative of CQ that possesses greater potency to inhibit autophagy and block tumor growth compared with HCQ (7). In agreement with this, CCOC cells treated with Lys05 accumulated more LC3-II compared with cells treated with HCQ (Supplementary Fig. S3A). Further cell viability assays showed that Lys05 was more cytotoxic than HCQ in all cell lines tested (Supplementary Fig. S3B). On the basis of this comparative potency analysis, we used Lys05 for all subsequent experiments.

To determine whether targeting the autophagy pathway could enhance sunitinib cytotoxicity, CCOC cells were treated with sunitinib and Lys05, and cell viability assays were performed. CCOC cells treated with sunitinib in combination with Lys05 resulted in a significant inhibition of cell viability under normoxia and hypoxia compared with sunitinib treatment alone (Fig. 3A and B). Under both normoxia and hypoxia, clonogenic survival assays demonstrated that the addition of Lys05 to sunitinib resulted in a greater degree of cytotoxicity compared with single-agent sunitinib in TOV21G and OVTOKO cells (Fig. 3C and D). OVMANA cells displayed the greatest sensitivity to single-agent therapies under

normoxia and hypoxia (Fig. 3C and D). To determine whether the effects of Lys05 were autophagy related, siRNA was used to knock down the essential autophagy gene *Atg5* in the presence or absence of sunitinib. Western blot analysis confirmed the reduction of Atg5 protein in TOV21G cells (Fig. 3E). We found that *Atg5*-siRNA in combination with sunitinib caused a significant impairment in cell viability compared with single-agent sunitinib (Fig. 3F). Under hypoxia, *Atg5*-siRNA also resulted in a significant reduction in cell viability when combined with sunitinib (Fig. 3G). Clonogenic cell survival assays showed that under normoxia, knockdown of Atg5 did not reduce survival of TOV21G cells nor did it sensitize cells to sunitinib, indicating that at least in this assay, cells do not rely on autophagy for survival under normoxic conditions (Fig. 3H and I). In contrast, cells treated with both *Atg5*-siRNA and sunitinib under hypoxia had a significant reduction in cell survival compared with single-agent sunitinib (Fig. 3H and I). Altogether, these results demonstrate that pharmacologic or genetic inhibition of autophagy under normoxia or hypoxia enhances the cytotoxicity of sunitinib in CCOC cells.

The above data suggest that the addition of Lys05 potentiates the anticancer activity of sunitinib *in vitro*. To evaluate whether the combination of sunitinib and Lys05 has synergistic activity in CCOC cells, the CI was calculated using the Chou and Talalay median effect principle (18). We found that sunitinib plus Lys05 resulted in a CI <1.0 for a number of different concentrations tested, indicating that sunitinib and Lys05 act synergistically in CCOC cells (Fig. 3J; Supplementary Fig. S4).

Sunitinib in combination with Lys05 induces apoptotic cell death

We next investigated whether the reduction in clonogenic survival and loss in cell viability following exposure to sunitinib and Lys05 was associated with increased apoptosis. As shown in Fig. 4A, caspase-3/7 activity was greater in the combination treatment compared with sunitinib treatment alone. OVMANA cells treated with Lys05 alone also showed a significant induction in caspase activity (Fig. 4A). Further western blot analyses revealed that the combination of sunitinib and Lys05 increased the levels of cleaved PARP, a substrate of caspase-3, confirming that the combination treatment induces apoptotic cell death (Fig. 4B).

Autophagy inhibition enhances sunitinib activity and blocks CCOC tumor growth *in vivo*

TOV21G cells displayed the least sensitivity to sunitinib under hypoxia compared with OVTOKO and OVMANA cells (Fig. 1B). On the basis of this result, we elected to first investigate whether the addition of Lys05 could potentiate the activity of sunitinib in the most resistant cell line that we tested under hypoxia. TOV21G cells were implanted subcutaneously into the flank of NOD/Scid mice. When tumor volume reached approximately 100 mm^3, mice were treated with saline, 20 mg/kg sunitinib, 20 mg/kg Lys05, or the combination of the two agents. Compared with the saline-treated group, mice treated with single-agent Lys05 or sunitinib, or the combination of the two agents resulted in a significant decrease in tumor volume (Fig. 5A and B). Importantly, mice in the cotreatment group displayed a 45% (P<0.01) and 54% (P<0.0001) reduction in tumor growth compared with mice treated with single-agent sunitinib or Lys05, respectively (Fig. 5A and B). To confirm these results, we also investigated whether the combination treatment was more

efficacious than single agents in the OVTOKO tumor model. Indeed, a significant reduction in relative tumor growth in the cotreatment group was observed compared with single-agent sunitinib or Lys05 (Fig. 5C).

To understand the mechanism by which the combination of sunitinib and Lys05 promotes tumor growth inhibition, we first examined autophagy levels in TOV21G tumor tissues. Tumors from sunitinib-treated mice showed decreased p62, whereas tumors from Lys05-treated mice showed increased p62, indicating that sunitinib and Lys05 can induce and block autophagy, respectively, *in vivo* (Fig. 5D). We next performed IHC analyses on TOV21G tumor sections using pimonidazole as a marker of hypoxia. Saline-treated mice displayed pimonidazole-positive regions, indicating that TOV21G tumors are hypoxic *in vivo* (Fig. 5E). Sunitinib treatment alone significantly reduced hypoxia-positive tumor regions compared with saline-treated mice, and addition of Lys05 did not further alter hypoxia within tumors (Fig. 5E). TOV21G tumor sections were further examined for cleaved caspase-3 and Ki-67 to determine whether alterations in apoptosis or proliferation could promote the reduction in tumor growth in the cotreatment group. Administration of sunitinib or Lys05 alone had little effect on cleaved caspase-3 staining; however, cleaved caspase-3 was significantly increased in the cotreatment group compared with sunitinib treatment alone (Fig. 5F). No significant difference in Ki-67 positivity was observed between any of the treatment groups, indicating that the mechanism of tumor regulation in the cotreatment group is mediated by apoptosis (Fig. 5G and F). Altogether, our data show that the addition of the autophagy inhibitor Lys05 potentiates the activity of sunitinib and impairs TOV21G and OVTOKO tumor growth *in vivo.*

Discussion

Several groups have demonstrated that CCOCs exhibit a marked upregulation of VEGF in addition to alterations in hypoxia response genes (10, 11, 30). Furthermore, upregulation of the PI3K/Akt/mTOR signaling pathway, specifically through mutations in PIK3CA and inactivating mutations in PTEN, is involved in the progression of CCOC (31). Although the multi-targeted profile of sunitinib has been shown to be efficacious for the treatment of RCC, PNET, and GIST, and case reports have indicated a potential benefit for sunitinib in CCOC, the response rates of CCOC in phase II trials has been low (16, 17). This suggests that inherent resistance mechanisms in CCOC may ultimately reduce the efficacy of sunitinib.

There have been conflicting reports of the effect of sunitinib on autophagy, highlighting that sensitivity to sunitinib-induced autophagy as well as autophagy inhibition varies depending on the tumor type (22–26). In our study, and consistent with these other reports, we found that sunitinib had different effects on autophagy depending on the CCOC cell line tested and on the presence or absence of oxygen. By Western blot analysis of endogenous LC3B-II levels, sunitinib induced autophagic flux in two of three cell lines tested under normoxia. Under hypoxia, however, sunitinib induced autophagic flux in OVTOKO cells only. The modest decrease in p62 levels observed in OVMANA cells following sunitinib treatment is consistent with the finding that at the concentrations tested, sunitinib may induce the formation of autophagosomal membranes but not flux through the system (28). Some of the

variation in sensitivity of CCOC cell lines observed under hypoxia may be due to cell line–dependent alterations in mitochondrial function, genetic background, or differential effects of combined hypoxia and sunitinib treatment, important factors that warrant further investigation (32). Despite the differences in autophagic flux, pharmacologic inhibition of autophagy using Lys05 or knockdown of *Atg5* sensitized CCOC cells to sunitinib *in vitro* under normoxia and hypoxia, highlighting that autophagy inhibition sensitizes CCOC cells to sunitinib. In addition, although we did observe some variability between the MTT and clonogenic survival assays, particularly in the siRNA-treated cells, this may reflect inherent differences in these assays. Despite these differences, our data show that even under low oxygen, autophagy inhibition sensitizes CCOC cells to sunitinib.

The TOV21G cell line displayed the least sensitivity to sunitinib under hypoxia. We therefore chose this cell line for further *in vivo* studies with the rationale that TOV21G may mimic CCOC tumors and therefore may have the highest resistance to sunitinib monotherapy (16, 17). Similar to our *in vitro* findings, tumor growth was significantly decreased in mice treated with Lys05 in combination with sunitinib, indicating that these drugs may work together in a cytotoxic manner. We were unable to compare tumor volume at later time points due to the size and aggressiveness of the untreated tumors that reached unacceptable clinical endpoints necessitating euthanasia. It is possible that alternate dosing and sequencing of sunitinib and Lys05 may also result in greater tumor cytotoxicity *in vivo*. However, we showed that daily administration of sunitinib and Lys05 resulted in significant decreases in tumor growth. Furthermore, immunohistochemical analyses revealed that the combination group had a greater amount of cleaved caspase-3, although no obvious differences in proliferation were observed. This indicates that the changes observed in tumor growth in the combination group are due to increased apoptosis rather than decreased proliferation. We also observed similar phenotypic features when sunitinib and Lys05 were coadministered in OVTOKO xenografts. It is important to point out that, to the best of our knowledge, there are no studies reporting the use of OVTOKO cells for *in vivo* tumor experiments. Within the first 5 days of implantation, OVTOKO tumor cells grew to 100 mm^3, but beyond this, the rate of growth spontaneously declined and tumors regressed, albeit incomplete. Despite the caveat of the OVTOKO model, the combination of sunitinib and Lys05 resulted in decreased relative tumor cell growth compared with either treatment alone. The growth properties of OVTOKO cells resulted in small tumors at the endpoint of the study and precluded further immunohistochemical analysis.

Short-term treatment of squamous cell carcinoma xenografts with sunitinib improved tumor oxygenation, decreased MVD, and prevented tumor hypoxia. In contrast, sunitinib treatment for up 2 weeks led to hypovascularity and a severe induction of hypoxia (13). We found that in the control saline group, TOV21G tumor xenografts displayed regions of hypoxia and that treatment with 20 mg/kg of sunitinib resulted in a significant decrease in hypoxia, which was not altered upon the addition of Lys05. In contrast, another study found a significant induction of hypoxia in A-07 and R-18 melanoma xenografts treated with 40 mg/kg of sunitinib (33). Thus, the induction of hypoxia following sunitinib treatment is likely cell line-, dose-, and duration dependent, and in some contexts may actually promote vascular normalization rather than attenuation. Further studies are needed to clarify these possibilities in CCOC.

Although HCQ demonstrated promising results in recent phase I/II clinical trials, the development of more potent autophagy inhibitors that display greater *in vivo* activity is urgently needed (2–6). Indeed, a recent report investigating sunitinib in combination with HCQ demonstrated that the MTD of HCQ, albeit through unknown mechanisms, inconsistently inhibited autophagy, thereby warranting the development of more potent and specific autophagy inhibitors (34). Here, we found that Lys05 was a more potent inhibitor of autophagy and was significantly more cytotoxic *in vitro* compared with HCQ, suggesting that Lys05 may have greater *in vivo* therapeutic efficacy (7). We cannot rule out the possibility that Lys05 may have other cytotoxic effects independent of autophagy. However, *Atg5* knockdown led to a similar increase in sensitivity to sunitinib when compared with Lys05.

In conclusion, the limited efficacy of sunitinib in clinical trials of CCOC may be due to inherent resistance mechanisms of CCOC, including hypoxia and autophagy. Nonetheless, our collective data show that sunitinib induces autophagy in CCOC and that genetic or pharmacologic inhibition of autophagy under normoxia or hypoxia potentiates the antitumor activity of sunitinib *in vitro* and *in vivo,* highlighting a potential new treatment combination for CCOC. Even within the CCOC histotype, we found that the sensitivity to sunitinib-induced autophagy as well as autophagy inhibition can vary depending on the cell line tested. Although the reason for these differences is not known, the molecular basis could involve multiple factors, including changes in metabolism, effects on the vasculature, and contribution of other cell types in the tumor environment, including immune cells.

Acknowledgments

The authors would like to thank Katy Milne and Heather Derocher for their help with tissue staining and IHC support and Sarah MacPherson for her helpful comments and suggestions. The authors would also like to thank Dr. Sharon M. Gorski for reagents and helpful comments on the manuscript.

Grant Support

This work was supported by the CIHR team grant GPG102167 and the Carraresi Foundation OVCARE Research Grants supported by the BC Cancer Foundation and VGH & UBC Hospital Foundation.

References

1. Yang ZJ, Chee CE, Huang S, Sinicrope FA. The role of autophagy in cancer: therapeutic implications. Mol Cancer Ther. 2011; 10:1533–41. [PubMed: 21878654]
2. Mahalingam D, Mita M, Sarantopoulos J, Wood L, Amaravadi RK, Davis LE, et al. Combined autophagy and HDAC inhibition: a phase I safety, tolerability, pharmacokinetic, and pharmacodynamic analysis of hydroxychloroquine in combination with the HDAC inhibitor vorinostat in patients with advanced solid tumors. Autophagy. 2014; 10:1403–14. [PubMed: 24991835]
3. Rangwala R, Chang YC, Hu J, Algazy KM, Evans TL, Fecher LA, et al. Combined MTOR and autophagy inhibition: phase I trial of hydroxychloroquine and temsirolimus in patients with advanced solid tumors and melanoma. Autophagy. 2014; 10:1391–402. [PubMed: 24991838]
4. Rangwala R, Leone R, Chang YC, Fecher LA, Schuchter LM, Kramer A, et al. Phase I trial of hydroxychloroquine with dose-intense temozolomide in patients with advanced solid tumors and melanoma. Autophagy. 2014; 10:1369–79. [PubMed: 24991839]

5. Vogl DT, Stadtmauer EA, Tan K-S, Heitjan DF, Davis LE, Pontiggia L, et al. Combined autophagy and proteasome inhibition: a phase 1 trial of hydroxychloroquine and bortezomib in patients with relapsed/refractory myeloma. Autophagy. 2014; 10:1380–90. [PubMed: 24991834]
6. Rosenfeld MR, Ye X, Supko JG, Desideri S, Grossman SA, Brem S, et al. A phase I/II trial of hydroxychloroquine in conjunction with radiation therapy and concurrent and adjuvant temozolomide in patients with newly diagnosed glioblastoma multiforme. Autophagy. 2014; 10:1359–68. [PubMed: 24991840]
7. McAfee Q, Zhang Z, Samanta A, Levi SM, Ma X-H, Piao S, et al. Autophagy inhibitor Lys05 has single-agent antitumor activity and reproduces the phenotype of a genetic autophagy deficiency. Proc Natl Acad Sci U S A. 2012; 109:8253–8. [PubMed: 22566612]
8. Chan JK, Teoh D, Hu JM, Shin JY, Osann K, Kapp DS. Do clear cell ovarian carcinomas have poorer prognosis compared to other epithelial cell types? A study of 1411 clear cell ovarian cancers. Gynecol Oncol. 2008; 109:370–6. [PubMed: 18395777]
9. Tan DSP, Miller RE, Kaye SB. New perspectives on molecular targeted therapy in ovarian clear cell carcinoma. Br J Cancer. 2013; 108:1553–9. [PubMed: 23558892]
10. Anglesio MS, George J, Kulbe H, Friedlander M, Rischin D, Lemech C, et al. IL6-STAT3-HIF signaling and therapeutic response to the angiogenesis inhibitor sunitinib in ovarian clear cell cancer. Clin Cancer Res. 2011; 17:2538–48. [PubMed: 21343371]
11. Stany MP, Vathipadiekal V, Ozbun L, Stone RL, Mok SC, Xue H, et al. Identification of novel therapeutic targets in microdissected clear cell ovarian cancers. PLoS One. 2011; 6:e21121. [PubMed: 21754983]
12. Spowart JE, Townsend KN, Huwait H, Eshragh S, West NR, Ries JN, et al. The autophagy protein LC3A correlates with hypoxia and is a prognostic marker of patient survival in clear cell ovarian cancer. J Pathol. 2012; 228:437–47. [PubMed: 22926683]
13. Matsumoto S, Batra S, Saito K, Yasui H, Choudhuri R, Gadisetti C, et al. Antiangiogenic agent sunitinib transiently increases tumor oxygenation and suppresses cycling hypoxia. Cancer Res. 2011; 71:6350–9. [PubMed: 21878530]
14. Zorn KK, Bonome T, Gangi L, Chandramouli GVR, Awtrey CS, Gardner GJ, et al. Gene expression profiles of serous, endometrioid, and clear cell subtypes of ovarian and endometrial cancer. Clin Cancer Res. 2005; 11:6422–30. [PubMed: 16166416]
15. Rauh-Hain JA, Penson RT. Potential benefit of Sunitinib in recurrent and refractory ovarian clear cell adenocarcinoma. Int J Gynecol Cancer. 2008; 18:934–6. [PubMed: 18081793]
16. Dancey J, Krzyzanowska MK, Provencher DM, Cheung WY, Macfarlane RJ, Alcindor T, et al. NCIC CTG IND.206: A phase II umbrella trial of sunitinib (S) or temsirolimus (T) in advanced rare cancers [abstract]. J Clin Oncol. 2015; 33(suppl) abstr 2594.
17. Chan J, Brady WE, Brown J, Shahin MS, Rose PG, Kim JH, et al. A phase II evaluation of sunitinib (SU11248) in the treatment of persistent or recurrent clear cell ovarian carcinoma: an NRG oncology / gynecologic oncology group study. Gynecol Oncol. 2015; 138:3. [PubMed: 26269805]
18. Chou T-C. Drug combination studies and their synergy quantification using the Chou-Talalay method. Cancer Res. 2010; 70:440–6. [PubMed: 20068163]
19. DeVorkin L, Go NE, Hou Y-CC, Moradian A, Morin GB, Gorski SM. The *Drosophila* effector caspase Dcp-1 regulates mitochondrial dynamics and autophagic flux via SesB. J Cell Biol. 2014; 205:477–92. [PubMed: 24862573]
20. Barth S, Glick D, Macleod KF. Autophagy: assays and artifacts. J Pathol. 2010; 221:117–24. [PubMed: 20225337]
21. Sorolla A, Yeramian A, Valls J, Dolcet X, Bergadá L, Llombart-Cussac A, et al. Blockade of NFκB activity by sunitinib increases cell death in bortezomib-treated endometrial carcinoma cells. Mol Oncol. 2012; 6:530–41. [PubMed: 22819259]
22. Santoni M, Amantini C, Morelli MB, Liberati S, Farfariello V, Nabissi M, et al. Pazopanib and sunitinib trigger autophagic and non-autophagic death of bladder tumour cells. Br J Cancer. 2013; 109:1040–50. [PubMed: 23887605]

23. Ikeda T, Ishii K-A, Saito Y, Miura M, Otagiri A, Kawakami Y, et al. Inhibition of autophagy enhances sunitinib-induced cytotoxicity in rat pheochromocytoma PC12 cells. J Pharmacol Sci. 2013; 121:67–73. [PubMed: 23269235]
24. Lin C-I, Whang EE, Lorch JH, Ruan DT. Autophagic activation potentiates the antiproliferative effects of tyrosine kinase inhibitors in medullary thyroid cancer. Surgery. 2012; 152:1142–9. [PubMed: 23158184]
25. Zhao Y, Xue T, Yang X, Zhu H, Ding X, Lou L, et al. Autophagy plays an important role in sunitinib-mediated cell death in H9c2 cardiac muscle cells. Toxicol Appl Pharmacol. 2010; 248:20–7. [PubMed: 20637791]
26. Abdel-Aziz AK, Shouman S, El-Demerdash E, Elgendy M, Abdel-Naim AB. Chloroquine synergizes sunitinib cytotoxicity via modulating autophagic, apoptotic and angiogenic machineries. Chem Biol Interact. 2014; 217:28–40. [PubMed: 24751611]
27. Tanida I, Ueno T, Kominami E. LC3 and autophagy. Methods Mol Biol. 2008; 445:77–88. [PubMed: 18425443]
28. Klionsky DJ, Abdelmohsen K, Abe A, Abedin MJ, Abeliovich H, Acevedo Arozena A, et al. Guidelines for the use and interpretation of assays for monitoring autophagy (3rd edition). Autophagy. 2016; 12:1–222. [PubMed: 26799652]
29. Saito Y, Tanaka Y, Aita Y, Ishii K-A, Ikeda T, Isobe K, et al. Sunitinib induces apoptosis in pheochromocytoma tumor cells by inhibiting VEGFR2/Akt/mTOR/S6K1 pathways through modulation of Bcl-2 and BAD. Am J Physiol Endocrinol Metab. 2012; 302:E615–25. [PubMed: 21878661]
30. Mabuchi S, Kawase C, Altomare DA, Morishige K, Hayashi M, Sawada K, et al. Vascular endothelial growth factor is a promising therapeutic target for the treatment of clear cell carcinoma of the ovary. Mol Cancer Ther. 2010; 9:2411–22. [PubMed: 20663925]
31. Dobbin ZC, Landen CN. The importance of the PI3K/AKT/MTOR pathway in the progression of ovarian cancer. Int J Mol Sci. 2013; 14:8213–27. [PubMed: 23591839]
32. Turcotte ML, Parliament M, Franko A, Allalunis-Turner J. Variation in mitochondrial function in hypoxia-sensitive and hypoxia-tolerant human glioma cells. Br J Cancer. 2002; 86:619–24. [PubMed: 11870546]
33. Gaustad J-V, Simonsen TG, Leinaas MN, Rofstad EK. Sunitinib treatment does not improve blood supply but induces hypoxia in human melanoma xenografts. BMC Cancer. 2012; 12:388. [PubMed: 22947392]
34. Melnyk N, Xie X, Koh DJY, Rajpal M, Moss RA, Gibbon D, et al. CTEP #8342 autophagy modulation with antiangiogenic therapy: a phase I trial of sunitinib (Su) and hydroxychloroquine (HCQ) [abstract]. J Clin Oncol. 2013; 31(suppl) abstr 2553.

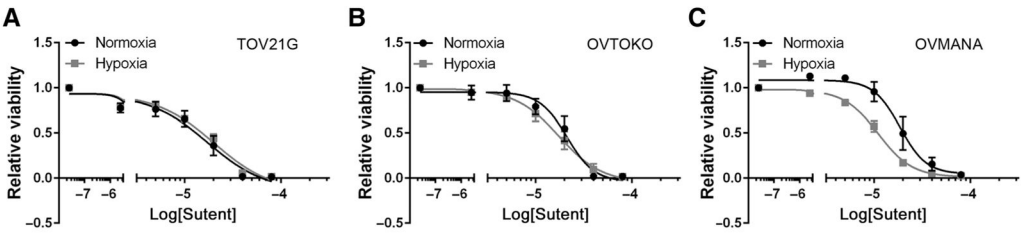

Figure 1.

CCOC cells are sensitive to sunitinib *in vitro*. **A–C,** TOV21G (**A**), OVTOKO (**B**), and OVMANA cells (**C**) were treated with sunitinib for 48 hours under normoxia (21% O_2) or hypoxia (1% O_2), and cell viability was measured by an MTT assay. Graph, average ± SEM ($n = 3$).

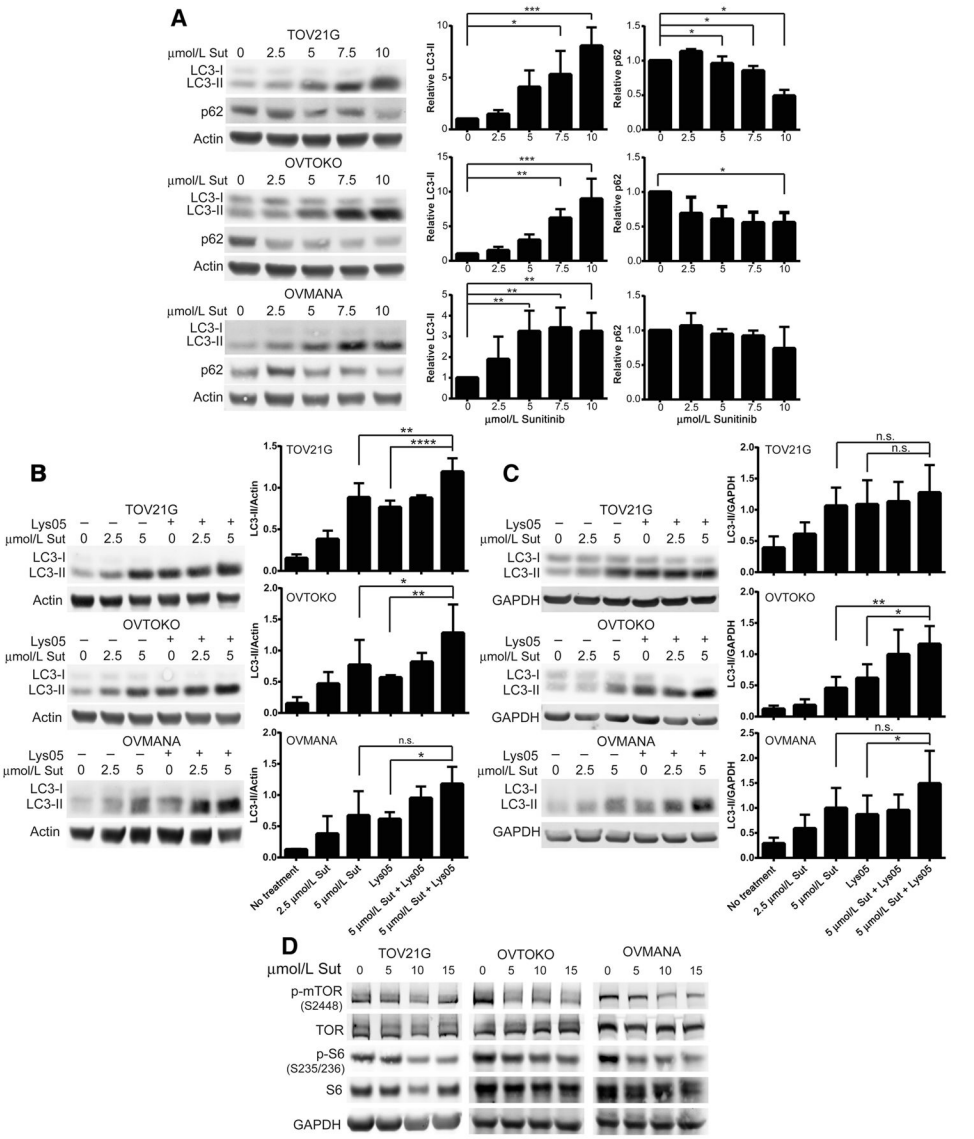

Figure 2.

Sunitinib induces autophagic flux in CCOC cells. **A,** CCOC cells were treated with sunitinib for 48 hours, and p62 and LC3 protein levels were assessed. Actin served as a loading control. Bar graphs show the average ± SD ($n = 3$; one-way ANOVA plus a Dunnet posttest)**.** **B** and **C,** CCOC cells were cultured under normoxia (**B**) or hypoxia (**C**) and treated with 2.5 or 5 µmol/L sunitinib for 48 hours in the presence or absence of saturating concentrations of Lys05. n.s., not significant. Actin or GAPDH served as a loading control. Bar graphs, average ± SD ($n = 3$–5; one-way ANOVA plus a Dunnet posttest). **D,** CCOC cells were serum starved for 24 hours, followed by the addition of serum in the presence or absence of the indicated concentrations of sunitinib for 1 hour. The phosphorylation status of mTOR and S6 ribosomal protein is shown ($n = 3$). GAPDH served as a loading control.*, $P<0.05$; **, $P<0.01$; ***, $P<0.001$; ****, $P<0.0001$. Sut, Sutent.

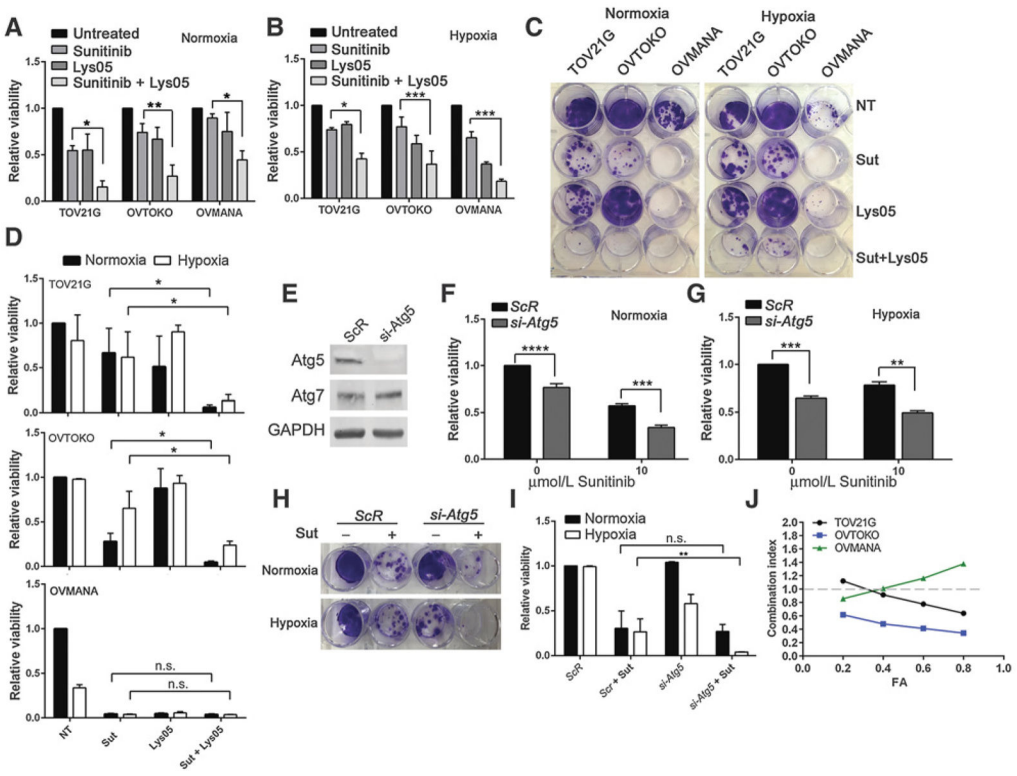

Figure 3.

Sunitinib and Lys05 synergistically impair viability in CCOC cell lines. **A** and **B,** CCOC cells were treated with 10 μmol/L sunitinib, 10 μmol/L Lys05, or the combination for 48 hours under 21% O_2 (**A**) or 1% O_2 (**B**). Cell viability was measured by an MTT assay. Graphs, average ± SEM ($n = 3$, Student t test). **C,** CCOC cells were treated with 10 μmol/L sunitinib, 10 μmol/L Lys05, or the combination for 48 hours under normoxia or hypoxia. Following treatment, media were replaced with fresh media, and cells were placed at 21% O_2 for 11 days. **D,** Cells were then stained with crystal violet and retained crystal violet was measured at 590 nm. Graphs, average ± SD ($n = 3$, Student t test). n.s., not significant. **E,** Representative Western blot showing Atg5 expression following scrambled (ScR) or Atg5 siRNA transfection into TOV21G cells. GAPDH served as a loading control. **F** and **G,** TOV21G cells were treated with siRNA targeting *Atg5,* or a ScR control in the presence or absence of 10 μmol/L sunitinib for 48 hours under normoxia (**F**) or hypoxia (**G**). Graphs, average ± SEM ($n = 3$, Student t test). **H,** ScR or *si-Atg5* TOV21G cells were treated with 10 μmol/L sunitinib for 48 hours under normoxia or hypoxia. Media were replaced with fresh media, and cells were allowed to recover under normoxia for 11 days. **I,** Cells were stained with crystal violet and retained crystal violet was quantified. Graph shows average ± SD ($n = 3$, Student t test). **J,** Cells were treated with sunitinib and Lys05 in a 2:1 ratio for 48 hours, and cell viability was measured. CI values for various fractions affected are shown. CI<1, synergistic interaction; CI > 1, antagonistic interaction; CI = 1 additive (dotted line). *, $P<0.05$; **, $P<0.01$; ***, $P<0.001$; ****, $P<0.0001$. Sut, Sutent.

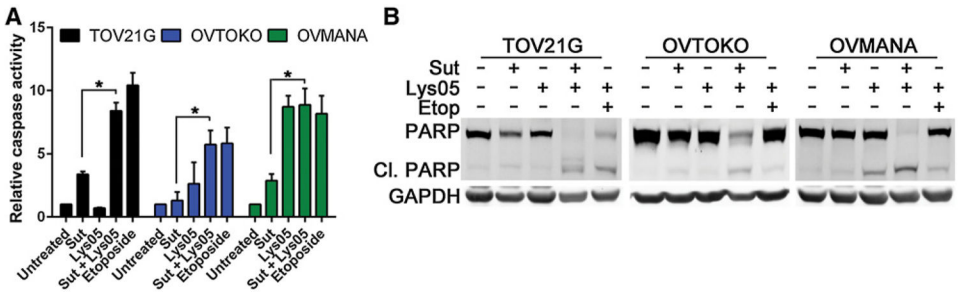

Figure 4.

Sunitinib and Lys05 induce apoptosis in CCOC. **A,** Caspase-3/7 activity was determined by treating CCOC cells with 10 μmol/L sunitinib, 10 μmol/L Lys05, or the combination for 48 hours. Etoposide served as a positive control. Graphs, average ± SEM (combined $n = 2$ of 3 independent experiments, Student t test; *, $P<0.05$). **B,** PARP cleavage was assessed following 10 μmol/L sunitinib, 10 μmol/L Lys05, or the combination of the two agents for 48 hours. Etoposide served as a positive control. GAPDH served as a loading control ($n = 3$). Sut, Sutent.

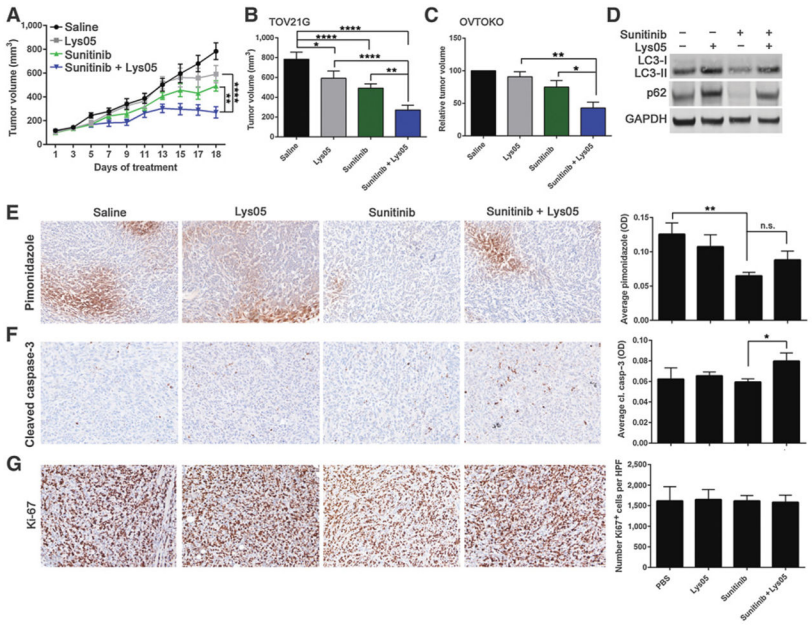

Figure 5.

Antitumor activity of sunitinib combined with Lys05 in TOV21G tumor xenografts. **A** and **B,** TOV21G cells (2×10^6) were implanted subcutaneously into the right flank of NOD/Scid mice. When tumor volume reached approximately 100 mm^3, mice were treated with saline, sunitinib (20 mg/kg), Lys05 (20 mg/kg), or the combination of the two agents for 18 days. Data are representative of 9 mice per treatment group ± SEM. Statistical significance was calculated using a two-way ANOVA with a Tukey multiple comparison posttest. **C,** Relative tumor volume of OVTOKO tumors 13 days post-saline, sunitinib (20 mg/kg), Lys05 (20 mg/kg), or combination treatment. Data are representative of 3 to 7 mice per treatment group ± SEM. Statistical analysis was calculated using a one-way ANOVA. **D,** TOV21G tumor lysates were pooled and analyzed for LC3-II and p62. GAPDH served as a loading control. **E** and **F,** Representative images of TOV21G tumor xenografts stained with pimonidazole (**E**) or cleaved caspase-3 (**F**). Graphs represent average pimonidazole or cleaved caspase-3 staining [optical density (OD)] from 3 to 5 high-power fields (HPF, 20×) representing 4 to 5 mice per treatment group ± SEM (one way ANOVA plus Sidak multiple comparison test, or Student *t* test). **G,** Representative images of TOV21G tumor xenografts stained with Ki-67. Graph represents average number of Ki-67^+ cells per 3 to 5 HPFs per treatment group (n = 4–5 mice per group) ± SEM. *, $P<0.05$; **, $P<0.01$; ****, $P<0.0001$.